Radiative thermal escape in intermediate band solar cells

A. Luque, A. Martí, E. Antolín, P. G. Linares, I. Tobías, and I. Ramiro
Instituto de Energía Solar, Universidad Politécnica de Madrid, Madrid 28040, Spain

To achieve high efficiency, the intermediate band (IB) solar cell must generate photocurrent from sub-bandgap photons at a voltage higher than that of a single contributing sub-bandgap photon. To achieve the latter, it is necessary that the IB levels be properly isolated from the valence and conduction bands. We prove that this is not the case for IB cells formed with the confined levels of InAs quantum dots (QDs) in GaAs grown so far due to the strong density of internal thermal photons at the transition energies involved. To counteract this, the QD must be smaller.

The intermediate band (IB) solar cell was proposed[1,2] to increase the efficiency of solar cells. In an IB solar cell, three energy bands allow electron-hole pair generation by two different mechanisms: by a single VB-CB (VB, valence band; CB, conduction band) transition and by successive VB-IB and IB-CB transitions. A very high detailed balance efficiency limit of about 63% versus 41% for an ordinary solar cell has been calculated.

Several groups[3–7] have realized these cells using the confined sates of InAs quantum dots (QD) in a GaAs matrix as an IB. It is known that this structure is not optimal in that the bandgaps are too small; however, it has permitted the study of the concept and the proof of its basic principles.[8,9] One of the shortcomings of present cells is thought to be the strong IB-CB thermal contact that prevents the CB quasi Fermi Level (QFL) from being above the IB QFLs, so preventing the appearance of a voltage (the difference between VB and CB QFLs) above the VB-IB sub-bandgap. This paper proves that, at room temperature, a strong thermal contact is produced by radiative interaction and that this interaction is enough to prevent substantial splitting of the QFLs in this material system.

A simple quantum analysis of the IB-CB optical transitions (also called intraband) has been presented.[10] It is based on the single band $\mathbf{k}\cdot\mathbf{p}$ method and uses a parallelepiped shape for the QD. The inaccuracy in assuming this shape is thought to be less important than the inaccuracy in determining the effective mass or the CB offset in the strained material. In this analysis, the different wavefunctions are labeled[10] with the three quantum numbers (n_x,n_y,n_z). For InAs QDs of size 16X16X6 nm^3 in a GaAs matrix and CB offset of 0.473 eV formed in the IB solar cell, labeled as SB in reference,[11] the bound states (BS) are represented in Figure 1 (see QD dimensions in the inset). When their energy is above the bottom of the matrix CB they are called virtual bound states (VBS).[12,13]

The BS within the GaAs bandgap constitute what we consider the IB. Its multilevel nature has been measured[14] and its influence in the IB cell limiting efficiency has been evaluated.[15]

The interest of the SB sample is that tunneling between QD layers has been prevented by using thick spacers and a voltage close to the GaAs bandgap —higher than the VB-IB bandgap— has been achieved at low temperature.[16]

For a single QD, the probability of (dipolar) photon absorption per unit time[17] (vol. II, p. 897) is (in SI units)

$$w_{|vN\mathbf{k}\rangle\to|v'(N-1)\mathbf{k}\rangle} = \frac{N_{ph,\mathbf{k}}}{\Omega}\frac{2\pi^2 e^2 E}{n_{ref}^2 h\varepsilon_0}\left|\langle\varphi|\,\boldsymbol{r}\cdot\boldsymbol{\varepsilon}\,|\varphi'\rangle\right|^2\delta(E_{v'}-E_v-E) \qquad (1)$$

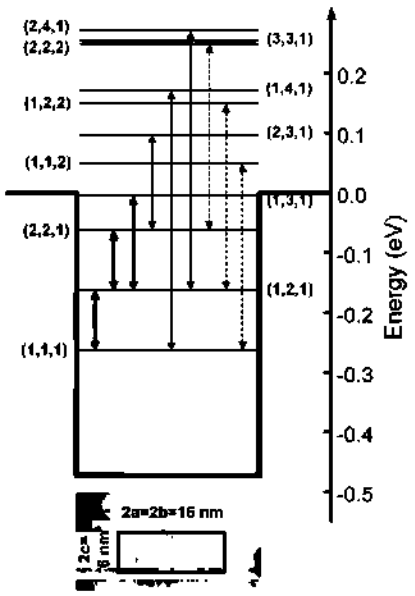

FIG. 1. Conduction band offset showing the CB edge and the relevant bound states due to the QD. Solid arrows are permitted generation under vertical or isotropic illumination; dotted are permitted under isotropic illumination only. Thicker lines show the main electron flow. Levels 121 collect the electrons received directly from the VB and via the levels 111 and 221 (the latter going downwards) and send them to the 131 level. Below, TEM photograph of a showing its dimensions.

where $\boldsymbol{\varepsilon}$ is the light polarization vector, n_{ref} is the refraction index of the medium, $N_{ph,\boldsymbol{k}}$ is the number of photons in the mode $\boldsymbol{k}$ and E, $E_{v'}$, E_v are the photon and initial and final electronic state energies. This expression represents the number of electron-hole pair generations per unit time due to absorption of photons in mode $\boldsymbol{k}$. If we set $N_{ph,\boldsymbol{k}}/\Omega = n_{ph}$ we are now taking into account the exciton generation by all modes with the same energy. For photon emission we must put $N_{ph,\boldsymbol{k}} + 1$ in the preceding equation.

For external illumination, the density of photons n_{ph} to be used in Eq. (1) can be related to the photon flux per unit time N_{ph} by $N_{ph} = (c/n_{ref})n_{ph}$. Furthermore, if F is the fractional coverage of the surface with QDs and there are N_l QD layers per unit length, the density of QDs per unit volume is $FN_l/4ab$ where $4ab$ is the QD cross-section. With this nomenclature the electron-hole generation rate per unit of volume and time is

$$\begin{aligned} g &= \int \frac{dN_{ph}}{dE}\frac{2\pi^2 e^2 E}{n_{ref}ch\varepsilon_0}\frac{\left|\langle\varphi|\,\boldsymbol{r}\cdot\boldsymbol{\varepsilon}\,|\varphi'\rangle\right|^2}{4ab}FN_l\delta(E_{v'}-E_v-E)dE \\ &= E_{line}N'_{ph}(E_{line})\frac{2\pi^2 e^2 E_{line}}{n_{ref}ch\varepsilon_0}\frac{\left|\langle\varphi|\,\boldsymbol{r}\cdot\boldsymbol{\varepsilon}\,|\varphi'\rangle\right|^2}{4ab}FN_l \end{aligned} \tag{2}$$

where $E_{line} = E_{v'} - E_v$. For weak absorption, assuming constant parameters in the IB thickness W_{IB} (including constant QFLs), the generated current density due to the external illumination is $J_{line}(E_{line}) = eW_{IB}g$. These values have to be doubled to account for the spin degeneracy of each state. Furthermore they have to be affected by the electron filling (Fermi function) factors of the state originating (f_{F1}) and receiving ($1\text{-}f_{F2}$) the electron.

The electrons are soaked in a gas of thermal photons, which are very abundant if the transition energy is low. The density of modes per unit of energy and volume is[18] $n'_{mo} = 8\pi n_{ref}^3 E^2/h^3c^3$. The Bose function f_B tells us the photon occupancy of each mode. Taking this into account the net recombination rate of electrons per unit of volume and time caused by the background photons is

TABLE I. Squared matrix elements normalized to 4ab for different transitions for vertical and isotropic illumination and the corresponding line energies according to reference.[10] The ratio of externally incident to internal ambient photon density is also calculated for the line energies for AM0 illumination of 0.136 W · cm^{-2} (0.0121 W · cm^{-2} below 0.726 eV).

	n_x, n_y, 1→2	n_x, n_y, 2→3	n_x, n_y, 3→4	n_x, n_y, 1→4	n_z, 1→2
Vertical	0.0212715	0.0190986	0.00461021	0.00016325	0
Isotropic	0.0106358	0.00954929	0.00230511	8.1626x10^{-5}	0.00112787
Energy (eV)	0.100503	0.158622	0.175218	0.434343	0.311947
External/internal ph. (1AM0 suns)	0.00009452	0.00054350	0.00091954	6.28179	0.088276

(by setting the thermal photon density and after some mathematical handling)

$$r_{net}(E_1, E_2, E_{F1}, E_{F2}) = (r - g) =$$

$$f_B \frac{8\pi n_{ref}^3 E_{line}^2}{h^3 c^3} \frac{2\pi^2 e^2 E_{line}}{n_{ref}^2 h\varepsilon_0} \frac{|\langle\varphi|\boldsymbol{r}\cdot\boldsymbol{\varepsilon}|\varphi'\rangle|^2}{4ab} F N_l f_{F,1}(1 - f_{F,2}) \left[\exp\left(\frac{E_{F,2} - E_{F,1}}{kT}\right) - 1\right] \tag{3}$$

where we have multiplied by the appropriate Fermi and Bose factors and we have assumed that the photons are in equilibrium with the surroundings (zero chemical potential) and not with the few excited QDs (chemical potential equal to $E_{F,2} - E_{F,1}$). According to this formula the flow of electrons goes, as expected, from the higher QFL to the lower one.

In the case studied in reference[10] the only permitted transitions must differ in one single quantum number and their initial and final values must be of different parity. Furthermore, the matrix element $\langle\varphi|\boldsymbol{\varepsilon}\cdot\boldsymbol{r}|\varphi'\rangle = \langle\varphi|x\cos\phi\sin\theta|\varphi'\rangle + \langle\varphi|y\sin\phi\sin\theta|\varphi'\rangle + \langle\varphi|z\cos\theta|\varphi'\rangle$ depends on the photon polarization, which is defined here by its Euler angles (ϕ, θ). The incident photons have a large variety of polarizations and the observed data results from averaging $|\langle\varphi|\boldsymbol{r}\cdot\boldsymbol{\varepsilon}|\varphi'\rangle|^2$. In the case of external vertical illumination $\theta = 0$ and this average is $(|\langle\varphi|x|\varphi'\rangle|^2 + |\langle\varphi|y|\varphi'\rangle|^2)/2$, but for symmetry reasons[10] only one of the two terms is not zero. In the case of isotropic illumination, as is the case for internal thermal photons, the average is $|\langle\varphi|x|\varphi'\rangle|^2/4 + |\langle\varphi|y|\varphi'\rangle|^2/4 + |\langle\varphi|z|\varphi'\rangle|^2/2$ and again only one term is not zero.

The matrix elements for different transitions are given in Table I. We can see also the ratio of photons from an external AM0 source at the extraterrestrial radiation level (0.136 W · cm^{-2}) and internal thermal photons at 300 K. For most levels this ratio is, in the absence of concentration, well below one.

The expression for the current of electrons pumped from the VB to an IB level of quantum numbers i, j, k is assumed to be

$$J_{Vijk}^{gr} \cong J_{Vijk}\left[1 - \exp\left(\frac{E_{Fijk} - E_{FV} - V_{balijk}}{kT}\right)\right] \tag{4}$$

where V_{balijk} is a parameter that reflects the balance of the pumping and recombination rates (note that this is just an unusual way of writing the diode equation).

Let us now consider the QFL for the different BS and VBS. The QFLs of the VBS (including the (131) level) are assumed to be in strong thermal contact with the CB and therefore all have the same QFL (E_{FC}). For the rest of the IB states we accept the separate QFLs, E_{F111}, E_{F121} and E_{F221}. Each state is filled by the electrons pumped from the valence band (VB) by high energy external photons with maximum current rates J_{V111}, J_{V121}, J_{V221} (modulated by the presence of empty sites in the IB levels) and is emptied by the net thermal generation (the opposite of the net thermal recombination in Eq. (3)) towards other BS and VBS. In addition it is emptied by pumping due to low energy external photons. The use of the maximum pumping rates J_{Vijk} assumes that $E_{Fijk} - E_{FV} << V_{balijk}$. This condition should be fulfilled near short circuit; in any case it represents an upper limit of the electron flow transferred to the IB levels.

The balance equations are

$$J_{V111}(1-f_{F111}) = 4J_{line}(E_{121}-E_{111})f_{F111}(1-f_{F121}) + 4J_{line}(E_{141}-E_{111})f_{F111}(1-f_{FC})$$
$$-4eW_{BI}r_{net}(E_{111}, E_{121}, E_{F111}, E_{F121}) - 4eW_{BI}r_{net}(E_{111}, E_{141}, E_{F111}, E_{FC})$$
$$-2eW_{BI}r_{net}(E_{111}, E_{112}, E_{F111}, E_{FC})$$

$$J_{V121}(1-f_{F112}) + 4eW_{BI}r_{net}(E_{111}, E_{121}, E_{F111}, E_{F121}) + 4J_{line}(E_{121}-E_{111})f_{F111}(1-f_{F121}) =$$
$$4J_{line}(E_{221}-E_{121})f_{F121}(1-f_{F221}) + 4J_{line}(E_{131}-E_{121})f_{F121}(1-f_{FC})$$
$$+4J_{line}(E_{421}-E_{121})f_{F121}(1-f_{FC}) + 2J_{line}(E_{122}-E_{121})f_{F121}(1-f_{FC}) \quad (5)$$
$$-4eW_{BI}r_{net}(E_{121}, E_{221}, E_{F121}, E_{F221}) - 4eW_{BI}r_{net}(E_{121}, E_{131}, E_{F121}, E_{FC})$$
$$-4eW_{BI}r_{net}(E_{121}, E_{421}, E_{F121}, E_{FC}) - 2eW_{BI}r_{net}(E_{121}, E_{122}, E_{F121}, E_{FC})$$

$$J_{V221}(1-f_{F221}) + 4eW_{BI}r_{net}(E_{121}, E_{221}, E_{F121}, E_{F221}) + 4J_{line}(E_{221}-E_{121})f_{F121}(1-f_{F221}) =$$
$$4J_{line}(E_{231}-E_{221})f_{F221}(1-f_{FC})$$
$$-4eW_{BI}r_{net}(E_{221}, E_{231}, E_{F221}, E_{FC}) - 2eW_{BI}r_{net}(E_{221}, E_{222}, E_{F221}, E_{FC})$$

Note that in these equations there are no J_{line} terms for external illumination associated to a change in the n_z quantum number because the corresponding matrix element is zero. Factors of 2 affect all terms discussed due to double spin. An additional factor of 2 (leading to 4) is included in the terms where a permutation in (n_x, n_y) leads to another totally symmetric state.

Note also we have not included transitions from the BS to the extended states of the CB. These transitions are expected to be small due to the negligible overlapping factor despite the many extended CB states. Anyway these transitions would only lead to a faster emptying of the IB states, reinforcing our arguments in this paper.

For this set to have a solution we must assume that E_{FC} is known. The E_{FC} QFL Fermi level changes its distance from the CB bottom (the energy origin throughout this paper) along the device (see e.g[19]). No VB QFL influence appears: this is only valid for the operation conditions mentioned above (near short circuit).

The terms $J_{V111}, J_{V121}, J_{V221}$ require the determination of the absorption coefficients of the VB-IB transitions; however, this is not important for our purpose. The sub-bandgap current measured[11] in the SB sample adjusted to the extraterrestrial radiation is 266 μA/cm^2. Of this current we have calculated (still unpublished[20]) that the currents absorbed by the (111), (121) and (221) levels are respectively 59.4, 17.8 and 19.0 μA/cm^2 when they are empty of electrons. However, only their order of magnitude is important for the conclusions drawn herein.

Detailed information of the transition currents between levels appears in Table II. The current pumped from the VB to the IB levels by the AM0 external illumination amounts to 64.6 $\mu A \cdot cm^{-2}$ and this current is transferred to the CB through the VBS. In the absence of the IR part of the AM0 external illumination (using a filter) the current pumped from the VB is smaller due to the higher occupation of the IB levels but the difference is negligible.

In this latter case, the (121) level receives 17.5 $\mu A \cdot cm^{-2}$ from the VB, as well as 27.2 $\mu A \cdot cm^{-2}$ from the (111) level (out of the 29.0 $\mu A \cdot cm^{-2}$ the (111) level receives from the VB) and 16.8 $\mu A \cdot cm^{-2}$ from the (221) level (out of the 26.1 $\mu A \cdot cm^{-2}$ it receives). It emits 61.4 $\mu A \cdot cm^{-2}$ to the (131) level assumed to be in the CB, out of the total 64.6 $\mu A \cdot cm^{-2}$ $\mu A \cdot cm^{-2}$ received. This means that most electrons pumped to the (111) and (221) levels reach the CB through the (131) (to which direct transitions are forbidden) via the (121) level. Note that the (121) QFL is the lowest among the IB QFLs, although the CB QFL is lowest. Similar behavior is observed with IR illumination.

In thick IB regions, charge neutrality has to be achieved at some value of the CB QFL so that a large region of charge neutrality appears, as required by the voltage boundary conditions.[21] This can be achieved by adding donors to the IB region (either to the barrier or QD material) to compensate

TABLE II. QFL positions (underlined) in eV with respect to the CB bottom and current density in $\mu A \cdot cm^{-2}$ of electron transference between levels due to AM0 illumination and internal thermal photons at 300 K. In each box the upper number is current density caused by external illumination and the lower number by thermal internal photons. Positive currents are upward transitions and negative downwards. WIB = 2.4 μm.

With external IR illumination													
IB/VBS Level	QFL (CB: -0.260)	VB	(111)	(121)	(221)	(131)	(112)	(231)	(122)	(141)	(222)	(241)	*Total*
(111)	-0.2618	29.04	0	**16.215**	0	0	0	0	0	1.6606	0	0	*17.876*
			0	**9.4826**	0	0	1.676	0	0	0.0058	0	0	*11.164*
(121)	-0.2619	17.461	**-16.22**	0	0.706	1.4785	0	0	0	0	0	0.0697	*-13.961*
			-9.483	0	**-17.56**	**58.39**	0	0	0.0699	0	0	0.0002	*31.422*
(221)	-0.2617	18.182	0	-0.706	0	0	0	0.0003	0	0	0	0	*-0.7056*
			0	**17.56**	0	0	0	1.3306	0	0	0.0016	0	*18.888*
Total		*64.683*	*-25.70*	*42.547*	*-16.85*	*59.868*	*1.676*	*1.3309*	*0.0699*	*1.6665*	*0.0016*	*0.0699*	*64.683*
Dopants/ QD	1.1105												
Without external IR illumination													
IB/VBS Level	QFL (CB: -0.260)	VB	(111)	(121)	(221)	(131)	(112)	(231)	(122)	(141)	(222)	(241)	Total
(111)	-0.2618	29.004	0	0	0	0	0	0	0	0	0	0	*0*
			0	**27.229**	0	0	1.7682	0	0	0.0061	0	0	*29.004*
(121)	-0.2618	17.46	0	0	0	0	0	0	0	0	0	0	*0*
			-27.23	0	**-16.79**	**61.409**	0	0	0.0735	0	0	0.0002	*17.46*
(221)	-0.2617	18.182	0	0	0	0	0	0	0	0	0	0	*0*
			0	**16.79**	0	0	0	1.387	0	0	0.0017	0	*18.182*
Total		*64.646*	*-27.23*	*44.023*	*-16.79*	*61.409*	*1.7682*	*1.387*	*0.0735*	*0.0061*	*0.0017*	*0.0002*	*64.646*
Dopants/ QD	1.1119												

the electrons appearing in the QDs. This density is usually of the order of the QD density. In the case presented in the table, the doping density normalized to the QD density is given for the QFL distribution resulting from the selected value of the CB QFL (-0.260 eV). This ratio is close to one (1.1105 and 1.1119 for the present and absent IR illumination). Insufficient doping may result in the need to compensate the charge with holes (dependent on the VB QFL) that may induce recombination not considered in this paper. However, the effect will be to reduce pumping from the VB; our conclusions therefore remain valid.

The use of larger bandgap materials permitting larger QD-barrier offsets will not change this situation very much if the QDs have the same size. In effect, a larger CB offset will certainly lower the position of the IB energy levels, but the difference between them will remain very much unchanged as can be easily understood by our model[10] (see Fig 2 in the reference). New states will appear forming a ladder with energy differences of 0.100-0.200 eV that can be climbed by absorption of internal thermal photons. The actual means of increasing the distance between levels is by reducing the lateral dimensions of the QDs; all dimensions must actually be small. This recommendation is that adopted in a recent paper of ours[22] for proposed QD IB materials.

In summary, we have calculated the density of thermally produced photons for the IB-CB energy range and have found that it is much higher than the density of photons resulting from one AM0 sun illumination (0.136 $W \cdot cm^{-2}$). Hence, the transfer of electrons among the IB levels and among them and the CB is very easy. As discussed in several papers,[1,2,19,21] this reduces the voltage and prevents the simultaneous occurrence of higher current and maintained voltage.

Furthermore, the illumination in the IB-CB range of energies is unnecessary and, if it is provided, becomes unnoticeable.

To solve these issues it is essential to produce smaller QDs so that the IB is formed preferably of a single level sufficiently separated from the CB as to be thermally isolated.

This work has been supported by the European Commission through the project IBPOWER (Grant 211640) and by the Spanish Ministry of Science and Innovation through the projects NANOGEFES: (Grant ENE2009-14481-C02-01) and DENQUIBAND (Grant PLE2009-0045).

[1] A. Luque and A. Martí, Physical Review Letters **78**, 5014–5017 (1997).
[2] A. Luque and A. Martí, Progress in Photovoltaics: Res. Appl. **9**, 73–86 (2001).
[3] A. Luque, A. Martí, C. Stanley, N. López, L. Cuadra, D. Zhou, and A. Mc-Kee, Journal of Applied Physics **96**, 903–909 (2004).
[4] S. M. Hubbard, C. D. Cress, C. G. Bailey, R. P. Raffaelle, S. G. Bailey, and D. M. Wilt, Applied Physics Letters **92**, 123512 (2008).
[5] V. Popescu, G. Bester, M. C. Hanna, A. G. Norman, and A. Zunger, Physical Review B **78**, 205321 (2008).
[6] S. A. Blokhin, A. V. Sakharov, A. M. Nadtochy, A. S. Pauysov, M. V. Maximov, N. N. Ledentsov, A. R. Kovsh, S. S. Mikhrin, V. M. Lantratov, S. A. Mintairov, N. A. Kaluzhniy, and M. Z. Shvarts, Semiconductors **43**, 514–518 (2009).
[7] R. Oshima, A. Takata, and Y. Okada, Applied Physics Letters **93**, 083111 (2008).
[8] A. Luque, A. Marti, N. Lopez, E. Antolin, E. Canovas, C. Stanley, C. Farmer, L. J. Caballero, L. Cuadra, and J. L. Balenzategui, Applied Physics Letters **87**, 083505–3 (2005).
[9] A. Marti, E. Antolin, C. R. Stanley, C. D. Farmer, N. Lopez, P. Diaz, E. Canovas, P. G. Linares, and A. Luque, Physical Review Letters **97**, 247701–4 (2006).
[10] A. Luque, A. Marti, E. Antolin, and P. Garcia-Linares, Solar Energy Materials & Solar Cells **94**, 2032–2035 (2010).
[11] E. Antolín, A. Marti, C. D. Farmer, P. G. Linares, E. Hernández, A. M. Sánchez, T. Ben, S. I. Molina, C. R. Stanley, and A. Luque, Journal of Applied Physics **108**, 064513 (2010).
[12] V. Popescu, G. Bester, and A. Zunger, Physical Review B **80**, 045327 (2009).
[13] G. Bastard, U. O. Ziemelis, C. Delalande, M. Voos, A. C. Gossard, and W. Wiegmann, Solid State Communications **49**, 671–674 (1984).
[14] E. Cánovas, A. Martí, N. López, E. Antolín, P. G. Linares, C. D. Farmer, C. R. Stanley, and A. Luque, Thin Solid Films **516**, 6943–6947 (2008).
[15] A. Luque, P. G. Linares, E. Antolín, E. Cánovas, C. D. Farmer, C. R. Stanley, and A. Martí, Applied Physics Letters **96**, 013501 (2010).
[16] E. Antolín, A. Martí, P. G. Linares, I. Ramiro, E. Hernández, C. D. Farmer, C. R. Stanley, and A. Luque, in *Proc.25 Photovoltaic Specialists Conference* (IEEE, Honolulu, 2010).
[17] A. Messiah, *Mécanique Quantique* (Dunod, Paris, 1960).
[18] A. Luque and A. Martí, in *Handbook of Photovoltaic Science and Engineering*, edited by A. Luque and S. Hegedus (John Wiley & Sons, Chichester, 2003), p. 113–151.
[19] I. Tobías, A. Luque, and A. Martí, Semiconductor Science and Technology **26**, 014031 (2011).
[20] A. Luque, A. Marti, E. Antolín, P. G. Linares, I. Tobías, I. Ramiro, and E. Hernandez, Solar Energy Materials & Solar Cells, to be published (2011).
[21] A. Luque and A. Marti, IEEE Transactions on Electron Devices **57**, 1201–1207 (2010).
[22] P. G. Linares, A. Marti, E. Antolin, and A. Luque, Journal of Applied Physics **109**, to be published (2011).